LOOK ACADEMIC PUBLISHERS
OPEN ACCESS

IEJME — MATHEMATICS EDUCATION
2016, VOL. 11, NO. 7, 2025-2046

Calculation of the Laser Beam Path through the Anisotropic Crystalline Lens

Abilhan U. Umbetov[a], Sania B. Zhumabaeva[a], Anuza Zhakenova[a], Bazargul S. Sadykova[a], Anar K. Tulegenova[a], Assel A. Aubakirova[a] and Saule Zh. Dzhaketova[a]

[a]Arkalyk State Pedagogical Institute named after Y. Altynsarin, KAZAKHSTAN.

ABSTRACT

Pursuant to the well-known theory of electromagnetic waves propagation in isotropic and anisotropic crystals, rigorous calculation of beam propagation in a system consisting of several anisotropic crystals, results in cumbersome expressions that are not suitable for engineering calculations and do not provide the possibility to study general properties of the two-component crystal-optical lenses. The authors developed an effective method of calculating propagation of electromagnetic waves through the two-component crystal-optical lenses based on uniaxial Iceland spar crystals with different orientations of the optical axes of the crystals in the lens components. Using a narrow beam method (paraxial approximation), the authors obtained an expression describing propagation of electromagnetic waves at the output of the two-component crystal-optical lenses. Based on the developed technique, propagation of electromagnetic waves through each section of crystal-optical lenses was calculated; the authors obtained expressions that are suitable for the analysis of properties in these systems as well as for engineering calculations. The paper presents a comprehensive experimental study of crystal-optical lenses in a split mode of electromagnetic waves at the output of crystal-optical lenses. Research results showed significant agreement between the results of calculations by formulas and experimental data.

KEYWORDS
Optical system; anisotropic crystals; double-focus lenses; paraxial approximation; Iceland spar

ARTICLE HISTORY
Received 30 January 2016
Revised 4 May 2016
Accepted 23 June 2016

Introduction

Computers are the main and universal means of information processing. However, high accuracy of calculations cannot be provided in many cases, because noises that appear at the input of the computer along with the processed signal make a significant contribution to output errors. The use of

CORRESPONDENCE Abilhan U. Umbetov ✉ umbetov.a@mail.ru

optical means (Demtröder, 2013; Alferov, 2014) may be preferable in cases that do not require high precision of calculations, but need efficiency, ease of use, small size, weight, power consumption and equipment cost.

Optical systems are particularly useful in processing a two-dimensional image information (Savin, Zubova & Manevitch, 2005). Keeping in mind that these calculations are made at the speed of light simultaneously for all pixels of the image, and the calculation time depends only on the time of the input signals and output of results, the performance of optical devices may exceed computer performance.

Taking into account rapid development of optical instrumentation, optical fiber communication, optical information recording and processing, further studies related to optical anisotropic crystals are required (Singh, Chaudhari & Pandey, 2016; Fabrizio & Rinaldi, 2015). Optical systems based on anisotropic crystals are of interest both in theoretical and in practical terms for the construction of electro-optical transmission devices, distribution and processing of information, in particular, laser measuring devices (Cattoor et al., 2014).

Background Paper

Crystalline systems provide the possibility to convert the frequency-modulated light into the amplitude - modulated; forming the desired optical filtering to optimize the processing of two-dimensional (optical) signals (Konoshonkin, Kustova & Borovoi, 2015; Porfiriyev, 2013; Chang, 2005). Two-component crystal-optical lenses at the output form the ordinary and extraordinary waves with varying degrees of polarization; their mixing by means of analyzers form different interference patterns being used in various laser measuring devices (Bazykin, 2014, Tarasov, Torshinina & Yakushenkov, 2014; Yang et al., 2015). The complexity of the calculations related to the propagation of electromagnetic waves in anisotropic medium (uniaxial and biaxial crystals) using the Maxwell's electromagnetic theory, was pointed out in several research works (Boyd, 2008; Barkovskii & Borzdov, 1975; Arminjon & Reifler, 2013). Using the covariant method within the framework of this theory provided detailed consideration of different characteristics of the reflected and refracted waves at the interface of uniaxial and biaxial crystals with the isotropic medium (Harris, 1963). Questions related to electrodynamics of anisotropic media (the construction of a one-dimensional wave equation and its solution matrix method) were discussed in the monograph M. Born & R. Wolf, (1997). Recent studies were marked by a new development in the method related to the analysis of the light propagation in an anisotropic medium, namely the particle-wave ratios of De Broglie, linking energy and momentum of a particle, with the frequency and wave vector respectively, were generalized to the case when the energy transfer and the wave distribution are directed (Mayer, 2007; Frieden, 2012; Khonina, 2013; Khonina, Karpeev & Alferov, 2012). Covariant method leads to the complicated general expressions, and its use in solving the problem of finding the direction of energy transfer in relation to the two-component crystal-optical systems is very difficult. In general, the problem does not imnply a strict analytical solution, the main difficulty is the need to take into account the parallelism of the wave vector $K=2\pi/\lambda$, describing transfer of the wave phase, and the energy-propagation direction $\overline{S} = [\overline{E}, \overline{H}]$, describing transfer of the wave energy (λ- wave length, E, H - vectors of the electric and magnetic fields). In this regard, one needs to provide the efficient method of calculating propagation of electromagnetic waves in crystal-optical lenses and to obtain the expression describing beam path at the output of the crystal-optical lenses.

In this article, propagation of the ordinary (o) and extraordinary (e) waves in an anisotropic dielectric medium with the boundary conditions for the bifocal lens (BL) is described by the simplest and quite general methods of geometrical optics in paraxial approximation, i.e., assuming infinitely narrow parallel beam incidence in different points of the input face of the anisotropic medium. This calculation method allows identifying all the basic properties of the studied BL and provides the possibility to compare calculation results with the experimental data

Research Purpose

The purpose of this study is to develop an efficient method for calculating propagation of electromagnetic waves through the two-component crystal-optical lenses based on uniaxial Iceland spar crystals with different orientations of the optical axes of the crystals in the lens components.

Research questions

The study aims at obtaining an expression that could provide the possibility to describe propagation of electromagnetic waves at the output of two-component crystal optical lenses using a narrow beam method (paraxial approximation); conducting a comprehensive experimental study of crystal-optical lenses in a split mode of electromagnetic waves at the output of crystal-optical lenses; making comparison of results obtained by calculations according to the formulas with the experimental data.

Method

Bifocal lenses (BL) with the binary structure based on the uniaxial crystals consisting of two glued plano-convex and plano-concave lens components with a different orientation of the optical axes, were described in detail by Y. Osipov (1973).

Assume that the circularly polarized wave extends through BL in the z direction. Given this choice of polarization state of this wave, "binding" the polarization vector to the optical axis of the crystal at the ACL input is negligible, which allows further unification of the theory for BL-1 and BL-2 (Figure 1).

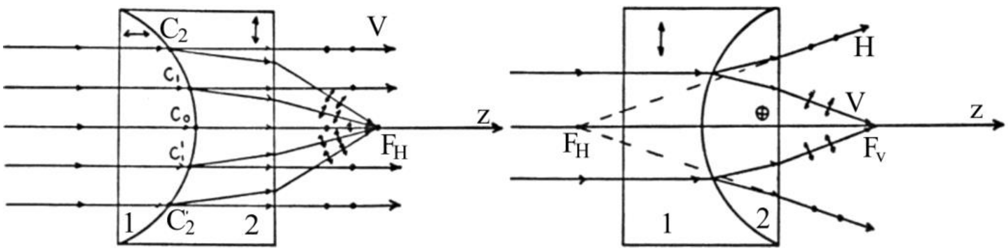

a) BL-1 b) BL-2

Figure 1. Two types of bifocal lenses

Assume that $z=0$ and $z=1$ present the left and right BL edges respectively, then the spherical boundary could be expressed by the following equation

$$x^2 + y^2 + (z - \sigma)^2 = R^2 \tag{1}$$

where σ - the distance from the coordinate origin to the center of the spherical BL surface. The interval between z = 0 and the spherical surface (1) is marked 1, and the rest is marked 2 (see Figure 2b). The convexity direction of the boundary is determined, naturally by the value sign δ. The directions of optical axis in ACL-1 and ACL-2 are specified by unit vectors $\vec{a}_1 = (1,0,0)$ and $\vec{a}_2 = (0, \sin\psi, \cos\psi)$, respectively, where ψ - the angle between $\vec{a}_2$ and the axis z. Assume that the narrow parallel beam of light strikes upon the left BL edge in the arbitrary point M_1 along the axis z (Figure 2a). Assume that M_1 has coordinates dcosφ, dsinφ, 0, where φ - the angle between the axis x and the radius-vector d, set off from the coordinate origin z = 0 to M_1. Hereafter, we assume that d ≪ R, where R – curvature of BL spherical boundary and the value $\left(\frac{d}{R}\right)^2$ is negligibly low.

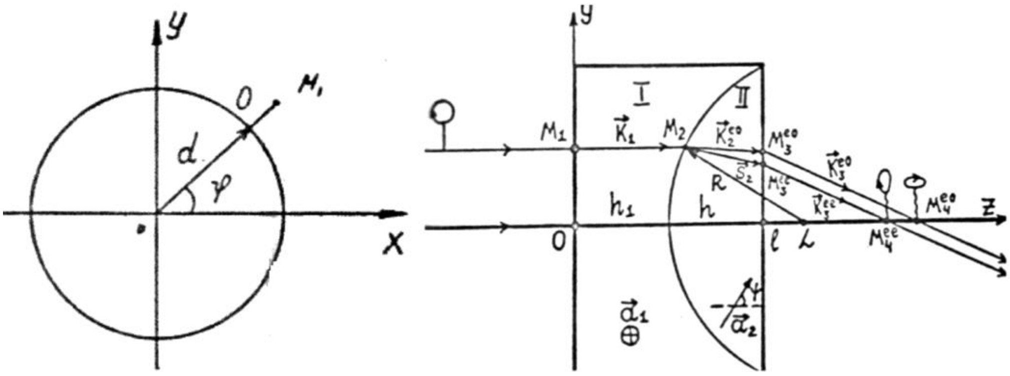

a) б)

Figure 2. Propagation of electromagnetic waves through the anisotropic crystalline lens made of **$CaCO_3$** uniaxial crystal.

The permittivity tensor in the principal axes of the crystal is diagonal and is set by the formula (2). Wave refraction index for o-wave in the intervals of I and II is identical and equals to n_0, and for the e – wave this index can be expressed as follows:

$$\varepsilon = \begin{pmatrix} \varepsilon & 0 & 0 \\ 0 & \varepsilon & 0 \\ 0 & 0 & \varepsilon \end{pmatrix} \tag{2}$$

$$\widetilde{n_e} = \frac{n_e}{\sqrt{1+\delta(\vec{k_i}\vec{a_i})^2}}, \tag{3}$$

where $\vec{k_i}$ (i = 1, 2) - unit wave vector in the intervals I and II respectively and $\delta = \frac{(n_e^2 - n_0^2)}{n_0^2}$.

Obviously, the unit wave vector for o – and e – waves in the interval I could be expressed as $\overrightarrow{k_1}$ (0,0,1), and it coincides with the direction of beam propagation. Mutual transformation of the o – and e – waves occurs on the spherical boundary of BL. The wave vector $\overrightarrow{k_2}$ in the interval II belongs (proceeding from the boundary conditions) to the plane, going through the axis z, defined by the angle φ, therefore, it can be expressed as follows:

$$\vec{k}_2 = \{\sin\alpha_2\cos\varphi; \sin\alpha_2\sin\varphi; \cos\alpha_2\} \tag{4}$$

where α_2 - the angle between $\overrightarrow{k_2}$ and the axis *z*.

Hereafter, the vector $\overrightarrow{k_2}$ and the angle d_2 will be marked by indexes (oo), (oe), (eo), and (ee). More specifically, (oo) indicates refraction of o – wave along with maintaining its polarization type, (oe) indicates transformation of the in-going wave (o) to the refracted (e) wave and so on. In general, four waves and four boundary conditions should be considered. It is obvious that α_2^{00}=0. The angle α_2^{0e} can be defined by the refraction law on the spherical surface:

$n_0^2[1-(\overrightarrow{k_1 n_1})^2] = \frac{n_e^2}{1+\delta(\overrightarrow{k_2^{0e} a_2})^2}\left[1-(\overrightarrow{k_2^{oe} n_1})^2\right]$, where $\overrightarrow{n_1} = \left\{\frac{d}{R}\cos\varphi; \frac{d}{R}\sin\varphi; -\sqrt{1-\frac{d^2}{R^2}}\right\}$ - normal unit vector. The beam cross point with the spherical boundary has the following coordinates $(d\cos\varphi, d\sin\varphi, \delta - \sqrt{R^2-d^2})$. Inserting values of the vectors $\overrightarrow{n_1}, \overrightarrow{k_1 k_2^{oe}}$ и $\overrightarrow{a_2}$ в (4), we obtain $\frac{n_0^2}{n_e^2}\frac{d^2}{R^2}(1+\delta\cos^2\varphi) = (\sin d_2^{oe} = \frac{d}{R})^2$, it follows that

$$d_2^{oe} = \frac{d}{R}\left(\frac{n_o}{n_e}\sqrt{1+\delta\cos^2\varphi} - 1\right) \tag{5}$$

The (eo) wave refraction law on the spherical surface will be expressed as follows:

$$\frac{n_e^2}{1+\delta(\overrightarrow{k_1 a_1})^2}\left[1-(\overrightarrow{n_1 k_1})^2\right] = \left[1-(\overrightarrow{n_1 k_2^{oe}})^2\right] n_o^2 \tag{6}$$

From (6) we obtain $d_2^{eo} = \frac{d}{R}\left(\frac{n_e}{n_o} - 1\right)$ (7)

The (ee) wave refraction law on the spherical surface will be expressed as follows: $\frac{n_e^2}{1+\delta(\overrightarrow{k_1 a_1})^2}\left[1-(\overrightarrow{n_1 k_1})^2\right] = \left[1-(\overrightarrow{n_1 k_2^{oo}})^2\right]\frac{n_e^2}{1+\delta(\overrightarrow{k_1 a_1})^2}$ (8)

Thus, inserting values of the vectors $\vec{\eta}, \vec{k}, \overrightarrow{k_2^{oe}}, \overrightarrow{a_2}$ и $\overrightarrow{a_1}$ we obtain

$$d_2^{oe} = \frac{d}{R}\left(\sqrt{1+\delta\cos^2\varphi} - 1\right) \tag{9}$$

Next, the wave unit vector of the beam, going out of BL will be expressed as follows:

$$\overrightarrow{\kappa_3} = \{\sin d_3\cos\varphi:\ \sin d_3\sin\varphi; \cos d_3\} \tag{10}$$

The (oo) wave is expressed as follows: $d_3^{00} = 0$. The wave (eo) refraction law on the boundary $z = \ell$ will be expressed as follows:

$$n_o^2\left[1-(\overrightarrow{n_1 k_2^{oe}})^2\right] = \left[1-(\overrightarrow{n_1 k_3^{oe}})^2\right] \tag{11}$$

where $\overrightarrow{n_2} = (0,0,1)$ – normal to the plane $z = \ell$. From the expression (11) we obtain

$$d_2^{eo} = \frac{d}{R}(n_e - n_0) \tag{12}$$

For the (oe) wave, the expression (11) will be as follows:

$$\frac{n_e^2}{1+\delta(\overrightarrow{k_2^{oe}}\overrightarrow{a_1})^2}\left[1-\overrightarrow{(n_2 k_2^{oe})}^2\right]=\left[1-\overrightarrow{(n_2 k_3^{oo})}^2\right] \tag{13}$$

From here, we obtain $\alpha_3^{oe}=\frac{d}{R}(n_0-\frac{n_e}{\sqrt{1+\delta\cos^2\psi}})$ (14)

The (ee) wave refraction law on the boundary $z=\ell$ will be expressed as follows:

$$\frac{n_e^2}{1+\delta\left(\overrightarrow{k_2^{ee}}\overrightarrow{a_2}\right)^2}\left[1-\left(\overrightarrow{n_2}\overrightarrow{k_2^{ee}}\right)^2\right]=\left[1-\left(\overrightarrow{n_2}\overrightarrow{k_2^{ee}}\right)^2\right] \tag{15}$$

From here, we obtain $\alpha_3^{ee}=\frac{d}{R}n_e(1-\frac{n_e}{\sqrt{1+\delta\cos^2\psi}})$ (16)

The formulas (15)-(16) allow finding the beam trajectories. Inserting the unit vector of the beam group speed $\vec{S}$ will result in the following expression:

$$\vec{S}=\mu_1\overrightarrow{a_2}+\mu_2\overrightarrow{k_2}; \qquad [\vec{S}]=1 \tag{17}$$

where μ_1 and μ_2 – coefficients.

From $(\vec{S}\vec{a})=\frac{\varepsilon^e(\vec{k}\vec{a})}{\sqrt{\varepsilon^{(0)2}+(\varepsilon^{(e)2}-\varepsilon^{(0)2})(\vec{k}\vec{a})}}$ we obtain

$$(\overrightarrow{sa_2})=\frac{n_e^2(\vec{k}_2\vec{a}_2)}{\sqrt{n_e^4(\overrightarrow{k_2}\overrightarrow{a_2})^2+n_o^4[1-(\overrightarrow{k_2}\overrightarrow{a_2})^2]}} \tag{18}$$

The coefficients μ_1 and μ_2 can be defined by taking the square of the equation (17) $\mu_1^2+\mu_2^2+2\mu_1\mu_2(\vec{\kappa}_2\vec{a}_2)=1$ (19)

From (18) and (19) we obtain:

$$(\overrightarrow{sa_2})=\mu_1+\mu_2(\vec{\kappa}_2\vec{a}_2)=\frac{n_e^2(\vec{k}_2\vec{a}_2)}{\sqrt{n_e^4(\overrightarrow{k_2}\overrightarrow{a_2})^2+n_o^4[1-(\overrightarrow{k_2}\overrightarrow{a_2})^2]}} \tag{20}$$

Therefore,

$$(\overrightarrow{sa_2})\,2=\mu_1^2+2\mu_1\mu_2(\vec{\kappa}_2\vec{a}_2)+\mu_2^2(\vec{\kappa}_2\vec{a}_2)=\frac{n_e^2(\vec{k}_2\vec{a}_2)}{\sqrt{n_e^4(\overrightarrow{k_2}\overrightarrow{a_2})^2+n_o^4[1-(\overrightarrow{k_2}\overrightarrow{a_2})^2]}} \tag{21}$$

Considering (20), we obtain

$$\mu_2=\frac{n_e^2}{\sqrt{n_e^4(\overrightarrow{k_2}\overrightarrow{a_2})^2+n_o^4[1-(\overrightarrow{k_2}\overrightarrow{a_2})^2]}} \tag{22}$$

and using the expression (20), we obtain

$$\mu_1=\frac{(n_e^2-n_0^2)(\vec{\kappa}_2\vec{a}_2)}{\sqrt{n_e^4(\overrightarrow{k_2}\overrightarrow{a_2})^2+n_o^4[1-(\overrightarrow{k_2}\overrightarrow{a_2})^2]}} \tag{23}$$

Inserting (22) and (23) in (17), we obtain

$$\vec{S}=\frac{[(n_e^2-n_0^2)(\vec{\kappa}_2\vec{a}_2)\vec{a}_2+n_0^2\vec{k}_2]}{\sqrt{n_e^4(\overrightarrow{k_2}\overrightarrow{a_2})^2+n_o^4[1-(\overrightarrow{k_2}\overrightarrow{a_2})^2]}} \tag{24}$$

The expression (24) for the beam vector $\vec{S}$ is required to determine the trajectory of the e – beam in BL.

Obviously, $\psi = 0$, which corresponds to BL-1 and $\psi = \frac{\pi}{2}$ – to BL-2.

Data, Analysis, and Results

Calculation of electromagnetic wave propagation through BL

For a uniaxial crystal of Iceland spar ($CaCO_3$) $n_0 > n_e$ and, consequently, from (14), under $\psi = \frac{\pi}{2}$, we obtain $\alpha_3^{oe} < 0$. This means that the o – beam in medium 1 exiting BL-2 deviates from the axis z, and therefore the parallel beam striking upon BL-2 will be divergent with regard to the given polarization. For the (eo) and (ee) beams, with regard to (12) and given $\psi = 0$ from (15) we obtain $\alpha_3^{oe} < 0\alpha_3^{ee} < 0$. This means that the (eo) and (ee) beams will cross the axis z at two different points. Thus, using the BL-1 provides realization of an interesting case related to the spatial division of a plane wave into two spherical waves with different foci along the axis z.

The unique property of ACL-1 related to creating two foci for the circularly polarized collimated beam is interesting in terms of optical measurements in the longitudinal direction (along z coordinate). Therefore, one should take a closer look at the location and structure of these foci.

First, let us consider the (eo) beam. The directing vector of the beam in the interval 2 is the vector $\vec{k}_2^{eo}$, and at the output of BL -1 $z > l$ – the vector $\vec{k}_3^{eo}$. Solution of the geometric problem related to the trajectory of the (eo) – beam shows that it crosses the axis z in a point M_4^{eo} (Figure 3) with the applicate $z_4^{eo} = l + F_{e0}$, where F_{e0} - focal length.

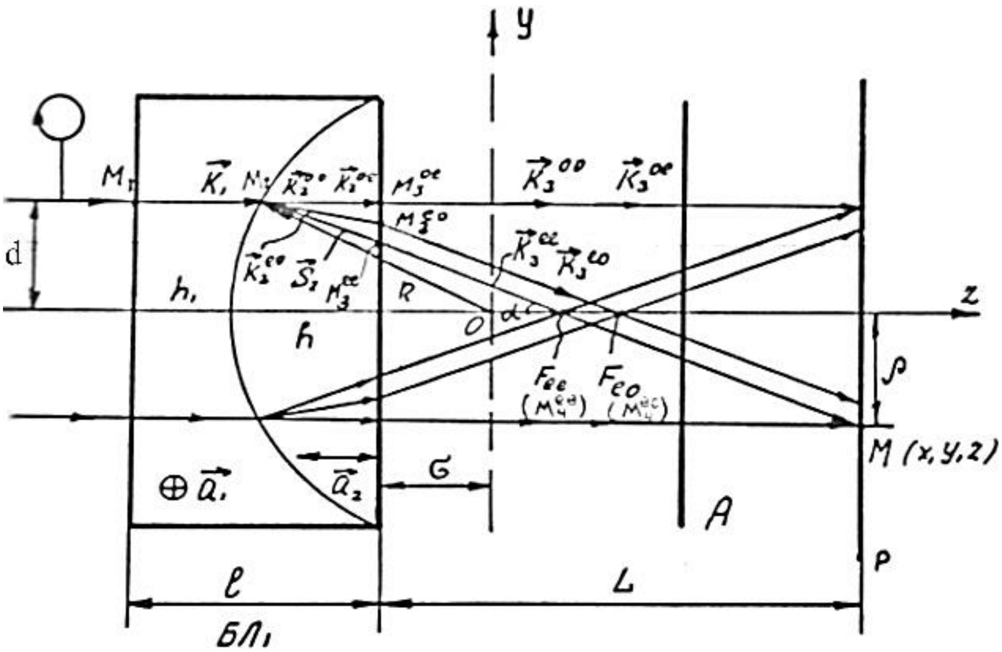

Figure 3. Electromagnetic wave propagation through a bifocal lens of BL-1 type

Defining the trajectory of the (eo) – beam involves finding points M_3^{eo} and M_4^{eo} by using the wave vectors $\vec{k}_2^{eo}$ and $\vec{k}_3^{eo}$, respectively. In the interval 2 – equation of the line $M_2M_3^{eo}$ is expressed as folows:

$$\frac{x-d\cos\varphi}{K_{2x}}=\frac{y-d\sin\varphi}{K_{2y}}=\frac{z-(\delta-\sqrt{R^2-d^2})}{K_{2z}} \tag{25}$$

From here we find coordinates of the point M_3^{eo}, assuming that z = l

$$x_3^{eo}=(l-h)k_{2x}+d\cos\varphi$$
$$y_3^{eo}=(l-h)k_{2y}+d\sin\varphi \tag{26}$$
$$z_3^{eo}=(l)$$

where $k_{2x}=\frac{d}{R}\left(\frac{n_e}{n_o}\right)\cos\varphi; k_{2y}=\frac{d}{R}\left(\frac{n_e}{n_o}\right)\sin\varphi; k_{2z}=[1-\left(\frac{d}{R}\right)^2(\frac{n_e}{n_o})^2]^{1\backslash 2};$

The equation of the line $M_3^{eo}M_4^{eo}$ could be expressed as

$$\frac{x-x_3^{eo}}{k_{3x}}=\frac{y-y_3^{eo}}{k_{3y}}=\frac{z-z_3^{eo}}{k_{3z}}, \tag{27}$$

where

$$k_{2x}=\frac{d}{R}(n_e-n_o)\cos\varphi; k_{2y}=\frac{d}{R}(n_e-n_o)\sin\varphi; k_{2z}=[1-\left(\frac{d}{R}\right)^2(n_e-n_o)^2]^{1\backslash 2};$$

In the focus (in the point M_4^{eo}) x=y=0, and from (28) taking into account the paraxial approximation, we obtain

$$Z_4^{eo}=Z_3^{eo}-\frac{k_{3x}}{k_{3z}}x_3^{eo}=l+\frac{R}{n_o-n_e}-\frac{l-h_1}{n_o} \tag{28}$$

From here we obtain

$$F_{eo}=\frac{R}{n_o-n_e}-\frac{h}{n_o} \tag{29}$$

where $h=l-h_1$ - height of the spherical segment in the interval 2, h_1 - distance between the left edge ($Z_0=0$) and the spherical boundary.

Focal length F_{ee} for the (ee)-beam could be found in a similar way, the difference is that the beam vector $\vec{S}_2^{ee}$, which determines energy transfer, is taken into account instead of the wave vector $\vec{k}_3^{ee}$ in the interval 2, At the output of BL-1, the vector $\vec{k}_3^{ee}$ is parallel to the vector $\vec{k}_3^{eo}$. Keeping in mind values of the vectors $\vec{a}_2$ and $\vec{k}_2^{ee}$ from (30), we express $\vec{S}_2^{ee}$ as:

$$S_{2x}^{ee}=\Delta_2^{-2\backslash 1}n_o\sin\alpha_2^{ee}\cos\varphi$$
$$S_{2y}^{ee}=\Delta_2^{-2\backslash 1}(n_e^2-n_o^2)\cos\psi\sin\psi+\Delta_2^{-2\backslash 1}n_o^2\sin\alpha_2^{eo}\sin\varphi\frac{n_o^2n_e^2}{\Delta_1} \tag{30}$$
$$S_{2z}^{ee}=\Delta_2^{-2\backslash 1}[\Delta_2+\frac{n_o^2n_e^2}{\Delta_1}(n_e^2-n_o^2)\sin\psi\cos\psi\sin\alpha_2^{eo}\sin\varphi$$

where $\Delta_1=n_e^4\cos^2\psi+n_o^4\sin^2\psi$; $\Delta_2=n_e^2\cos^2\psi+n_o^2\sin^2\psi$

From (30) it follows that $\vec{S}_2^{ee}$ belongs to a plane, which could be defined by the angle φ and the axis Z only provided $\psi = 0$ and $\psi = \frac{\pi}{2}$. Given the angles $\psi \neq 0, \frac{\pi}{2}$ (ee) – beam does not cross the axis z and BL-1 does not have focusing properties. Provided $\psi = 0$, we obtain

$$S_{2x}^{ee} = (\frac{n_o}{n_e})^2 \cos\varphi \sin\alpha_2^{ee}$$

$$S_{2y}^{ee} = (\frac{n_o}{n_e})^2 \sin\varphi \sin\alpha_2^{eo} \tag{31}$$

$$S_{2z}^{ee} = 1$$

Provided $\psi = \frac{\pi}{2}$, we obtain $S_{2x}^{ee} = S_{2y}^{ee} = 0$; $S_{2z}^{ee} = 1\alpha_2^{ee} = 0$. Therefore, provided $\psi = 0$ the (ee)-beam is focused. In order to determine focal length F_{ee} one needs to find coordinates of $M_3^{eo}$and M_4^{eo}. Whereas the line $M_2M_4^{ee}$ is defined by the equation $\frac{x_3^{ee} - d\cos\varphi}{S_{2x}} = \frac{y_3^{ee} - d\sin\varphi}{S_{2y}} = \frac{z - (\delta - \sqrt{R^2 - d^2})}{S_{2z}}$

(32)

coordinates of the point M_3^{ee} we express as

$$X_3^{ee} = (l - h)S_{2x} + d\cos\varphi$$

$$Y_3^{ee} = (l - h)S_{2x} + d\sin\varphi \tag{33}$$

$$Z_3^{ee} = l$$

Accordingly, from the equation of the line $M_3^{eo}M_4^{eo}$

$$\frac{x - x_3^{ee}}{k_{3x}} = \frac{y - y_3^{ee}}{k_{3y}} = \frac{z - z_3^{ee}}{k_{3z}} \tag{34}$$

For the applicate of the point M_4^{ee} we have $Z_4^{ee} = Z_3^{ee} - \frac{K_{3z}}{K_{3x}} X_3^{ee}$ or

$$Z_4^{ee} = l + \frac{R}{n_o - n_e} - \frac{(l - h_1)}{n_e^2} n_0 \tag{35}$$

and the focal length of the (ee) wave will be expressed as follows

$$F_{ee} = Z_4^{ee} - l = \frac{R}{n_o - n_e} - h\frac{n_o)}{n_e^2} \tag{36}$$

From (29) and (36) we obtain the distance between the foci:

$$\Delta F = F_{eo} - F_{ee} = h\frac{n_o^2 - n_e^2}{n_o n_e^2} \tag{37}$$

The expression (37) shows that the distance between the foci depends only on the h value and birefringent properties of the crystal, which forms the basis of BL-1.

In the case of a negative crystal ($CaCO_3$), $n_o > n_e F_{ee} < F_{eo}$. In the case of a positive crystal (SiO_2), when $n_o < n_e$, the (eo) beam focus is located closer ($F_{ee} > F_{eo}$). For the BL made of $CaCO_3$ provided h = 5,35 mm and R = 24,7 mm, given laser radiation with λ = 632,8 nm, $n_0 = 1{,}65504$, $n_e = 1{,}48490$, the calculation according to (29) and (37) provides $F_{ee} = 141{,}3$ мм, $F_{eo} = 142{,}1$ mm and $\Delta F = 0{,}8$ m, which is qualitatively correlated with the experiment (see Figure 4).

The above consideration implies that ACL-1 focuses part of the parallel beam at two points, defined by the expressions (29) and (37), whereas BL-2 fixes it in one point (29). It should be noted that two parallel beams are formed in the output of BL-1 along with the intact (circular) polarization of the incident beam.

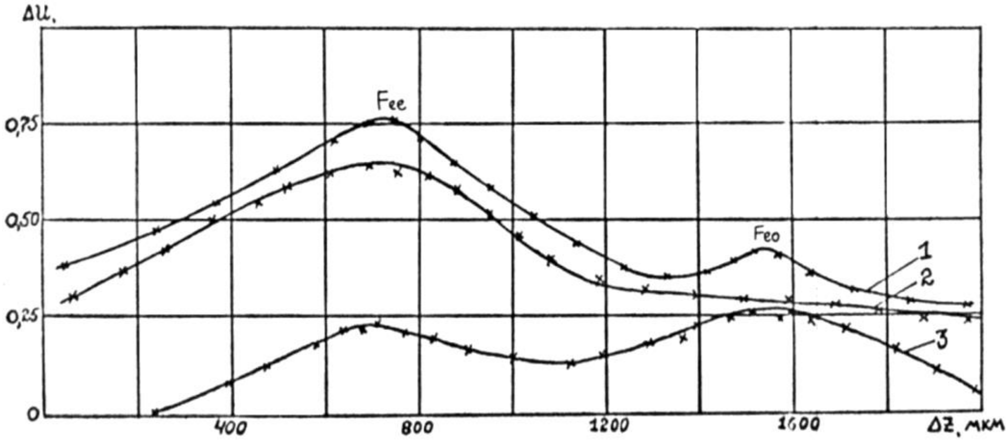

Figure 4. Light intensity distribution in the focal plane of BL-1 (in foci $\mathbf{F_{ee}}$ and $\mathbf{F_{eo}}$): 1 - without analyzer (A), 2 - under A||$\overrightarrow{\mathbf{a_1}}$ (axis of the analyzer is parallel to the optical axis of the crystal $\overrightarrow{\mathbf{a_1}}$), 3 - under A$\perp\overrightarrow{\mathbf{a_1}}$ (axis of the analyzer is perpendicular to the optical axis of the crystal $\overrightarrow{\mathbf{a_1}}$)

Figure 4 shows the experimental curves of the light flow (1) intensity distribution along the axis z in the focal plane $M_4^{ee}$and M_4^{eo} БЛ-1. The curve 1 was obtained through PMT (input diaphragm – 3 um), which was moved along the axis z by horizontal comparator of IZA-2 type. Setting the analyzer parallel to $\overrightarrow{a_1}$ (curve 2) and perpendicular to $\overrightarrow{a_1}$ (curve 3), the authors determined largely orthogonal-elliptical state of the light flux polarization at the foci F_{ee} and F_{eo}. Experimental measurements of the polarization selection in the ACL-1 foci cause difficulties due to the length of the test beams along the axis z. As regards the intensity of $I_{ee}$and I_{eo} in the foci of BL-1, they are not identical as shown by Figure 4. According to relevant calculations, their ratio should make $\frac{I_{ee}}{I_{eo}} = 3$, which is qualitatively correlated with the experiment (curve1).

It is known that the wave reversibility is not observed in two or more polarizing systems, in other words, wave polarization is not kept intact during direct and reverse propagation through the system (Khonina, 2013). Therefore, it seems expedient that the problem of the reverse propagation of the parallel light beam through the BL be separately considered. For BL-1, the e and o-beams are indistinguishable at normal incidence to the area 2, as they propagate along the optical axis $\overrightarrow{a_2}$. This means that the o-beam propagating to the left of BL-1 keeps its direction, and the e-beam crosses the axis z. Considering the focus of e-beam, the formula (29) demonstrates that at normal incidence of the beam having cylindrical form to the right of the BL-1, with radius r_0 at the output of BL-1 the beam is elliptically contoured (Khonina, Karpeev & Alferov, 2012). In this case, the wave vector in the interval 2 of ACL-1 is determined by the unit vector as $\overrightarrow{K_1}$=(0,0,-1), and the optical axes of BL-1 are determined by the unit vectors, namely, $\overrightarrow{a_1}$ =(1,0,0); $\overrightarrow{a_2}$=(0,0,1). The unit normal to the spherical surface in point M_2:

$$\vec{n}_1 = \{\frac{d}{R}\cos\varphi;\quad \frac{d}{R}\sin\varphi;\quad -\sqrt{1-\frac{d^2}{R^2}}\}$$

The wave vector in the interval 1 of ACL-1 could be expressed as follows:

$$\vec{K}_2 = \{\mathrm{sind}_2\mathrm{cos}\varphi; \quad \mathrm{sind}_2\mathrm{sin}\varphi; \quad -\mathrm{cosd}_2\}.$$

Obviously, for the (o)-beam d_2^0= 0, d_3^0= 0. The refraction law for the e-beam on the spherical surface is expressed as follows:

$$n_0^2\left[1-\left(\vec{k}_1\vec{n}_1\right)^2\right] = \frac{n_e^2}{1+\delta\left(\vec{k}_2\vec{n}_1\right)^2}\left[1-\left(\vec{k}_1\vec{n}_1\right)^2\right] \tag{38}$$

Thus, upon inserting values of the vectors $\vec{k}_1$,$\vec{n_1}$, $\vec{k}_2$ and $\vec{a_1}$, we obtain

$$d_2^e = \frac{d}{R}\left(1-\frac{n_o}{n_e}\right) \tag{39}$$

On the boundary z=0 the refraction law for the e-beam is expressed as follows:

$$\frac{n_e^2}{1+\delta\left(\vec{k}_2\vec{n}_1\right)^2}\left[1-\left(\vec{k}_1\vec{n}_1\right)^2\right] = \left[1-\left(\vec{k}_1\vec{n}_1\right)^2\right] \tag{40}$$

where $\vec{n_2}$=(0,0,1)-normal to the plane z=0. From (39) we obtain

$$d_3^e = \frac{d}{R}(n_e - n_o) \tag{41}$$

The beam vector in the interval 1 of ACL – 1 will have the following expression (with regard to the expression (24)

$$\vec{S}_2 = \frac{n_e^2-n_o^2}{n_o^2} sind_2^e cos\varphi \vec{a}_1 + \vec{K}_2 \tag{42}$$

From here we obtain

$$\begin{gathered} S_{2x} = \frac{n_e^2}{n_o^2} sind_2^e cos\varphi \\ S_{2y} = sind_2^e sin\varphi \\ S_{2z} = 1 \end{gathered} \tag{43}$$

We find coordinates of the e-beam intersection points in the plane Z=0. The coordinates of M_2 can be expressed as follows $(dcos\varphi,\ dsin\varphi 6\ \delta - \sqrt{R^2-d^2})$

$$\frac{x_3 - dcos\varphi}{S_{2x}} = \frac{y_3 - dsin\varphi}{S_{2y}} = \delta - R = h \tag{44}$$

From here we obtain

$$\begin{gathered} x_3 = h_1\frac{n_e^2}{n_0^2}\left(1-\frac{n_0}{n_e}\right)\frac{d}{R}cos\varphi + dcos\varphi \\ y_3 = h_1\left(1-\frac{n_0}{n_e}\right)\frac{d}{R}sin\varphi + dsin\varphi \\ \mathrm{z}_3 = 0 \end{gathered} \tag{45}$$

The equation related to the e-beam propagation in output of ACL-1 can be expressed as follows:

$$\frac{x-x_3}{K_{3x}} = \frac{y-y_3}{K_{3y}} = \frac{z-z_3}{K_{3z}} \tag{46}$$

From here we obtain

$$\begin{gathered} x = x_3 + (z-z_3)K_{3x} \\ y = y_3 + (z-z_3)K_{3y} \end{gathered} \tag{47}$$

Taking into account (45) and (41) and proceeding from the assumption that d=r_0, from the expression (47) we obtain

$$x = \left[h_1 \frac{n_e^2}{n_0^2}\left(1 - \frac{n_0}{n_e}\right) + R + z(n_e - n_0)\right]\frac{r_0}{R} cos\varphi = Acos\varphi$$

$$y = \left[h_1\left(1 - \frac{n_0}{n_e}\right) + R + z(n_e - n_0)\right]\frac{r_0}{R} sin\varphi = Bsin\varphi \qquad (48)$$

From (48) we obtain the obtain the desired ellipse equation (intensity distribution in the foci $F_{oe}$and F_{eo}) $\frac{X^2}{A^2} + \frac{Y^2}{B^2} = 1$ (49)

where

$$A = \left[h_1 \frac{n_e^2}{n_0^2}\left(1 - \frac{n_0}{n_e}\right) + R + f(n_e - n_0)\right]\frac{r_0}{R}$$

$$B = \left[h_1\left(1 - \frac{n_0}{n_e}\right) + R + f(n_e - n_0)\right]\frac{r_0}{R} \qquad (50)$$

and f=z.

As can be seen from (50), the parameters of the ellipse A and B do not simultaneously make zero at any f. Strictly speaking, this means that there is no focus. However, either at A=0, or at B=0 the ellipse turns into in a vertical or horizontal line segment with the following values of f:

$$f_1 = \frac{R}{n_0 - n_e} - h_1 \frac{n_e}{n_0^2}$$

$$f_2 = \frac{R}{n_0 - n_e} - \frac{h_1}{n_e} \qquad (51)$$

From (51) it follows that $f_1 > f_2$ and

$$\Delta f = f_1 - f_2 = \left(\frac{1}{n_e} - \frac{n_e}{n_0^2}\right) h_1 = \frac{n_0^2 - n_e^2}{n_e n_0^2} h_1 \qquad (52)$$

Dimensions of the vertical and horizontal "focal segments" are equal to

$$\Delta l = 2\frac{r_0}{R}\frac{n_0^2 - n_e^2}{n_e n_0^2} h_1 = 2\Delta f \frac{r_0}{R} \qquad (53)$$

This phenomenon is associated with the phenomenon of astigmatism, in which the beam corresponds to the wave surface of double curvature. In this case, the intersection of the rays occurs in multiple points located on the two mutually perpendicular rectilinear segments. The distance between the "focal segments" Δf is called the astigmatic difference. The normal cross section of the beam between the "focal segments" has the form of arc, and it is called the circle of least confusion. With the reduction of the astigmatic difference Δf the length of the "focal segments" and the radius of the circle of least confusion diminish. It should be emphasized that in this case one can speak only about the extended focal plane, which dimensions are determined by the expressions (52) and (53).

The above picture of the light beam passage is also valid for the BL-2 for the (oe)-wave as the interval 2 contains the o-beam, which after refraction at the spherical surface transforms into the e-beam. However, in contrast to the BL-1, BL-2 also creates the divergent (eo) - beam resulting from the transformation of the e-beam (from the interval 2) into the o-beam (in the interval 1).

Discussion and Conclusion

Angular dividing characteristics between the o and e-beams in BL

The two-component crystal optical lenses of BL-1 and BL-2 types have a noticeable effect, which implies beam dividing (picture doubling). Unlike the well-known systems (Konoshonkin, Kustova & Borovoi, 2015; Harris, 1963), the dividing angle (the angle between (o) and (e) beams) at the BL output has a strong nonlinear dependence on the angle of incidence (Khonina, Karpeev & Alferov, 2012). This property of the BL-1 and BL-2 lens types provides several new features in terms of their application.

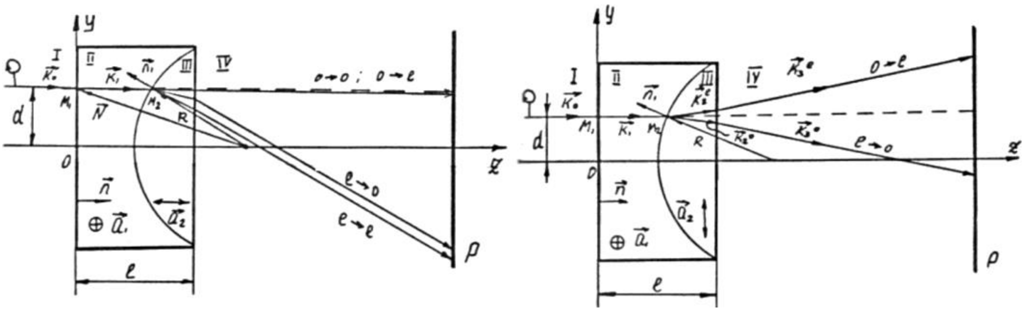

Figure 5. Beam propagation through BL-1 (a) and BL-2 (b)

Figure 5 shows beam propagation through BL-1 and BL-2. Provided normal incidence of the beam on the entrance face of the lens, the wave vectors of o- and e-waves at the output of ACL-1 and ACL-2 provide the following angles to the axis z: for BL-1:

$$d_3^{oo} = d_3^{oe} = 0$$
$$d_3^{eo} = \frac{d}{R}(n_e - n_o)$$
$$d_3^{ee} = \frac{d}{R}(n_e - n_o) \tag{54}$$

for BL-2:

$$d_3^{oo} = d_3^{ee} = 0$$
$$d_3^{oe} = \frac{d}{R}(n_e - n_o)$$
$$d_3^{eo} = \frac{d}{R}(n_e - n_o) \tag{55}$$

As could be seen from (54) and (55), given normal incidence of the beam to the entrance face of ACL-1 and ACL-2 the wave deflection angle at the output of these lenses (relating to the initial direction) is linearly dependent on the radius vector d (Figure 6).

In the case of the beam incidence on the entrance face of BL-1 and BL-2 at an arbitrary angle, the calculation of doubling the beam (picture), the paraxial approximation provides bulky and uncomfortable for the physical analysis of the results. In this case, double beam (image) in the lenses CLA-1 and CLA-2 will be considered upon the previously developed techniques (Mayer, 2007), in relation to the prisms of variable angle doubling (DPPUD), consisting of two wedges uniaxial crystal glued hypotenuse side, with different orientation axes in the wedge components.

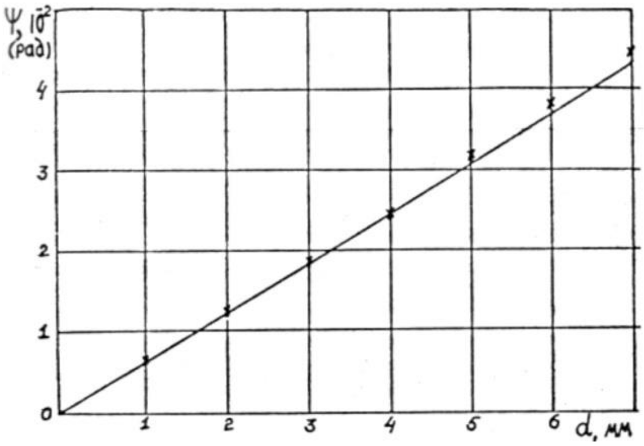

Figure 6. The dependence of the dividing angle in the ACL-1 and ACL-2 on the radius - vector d

Direction of the optical axes of the lenses could be defined by the vectors $\overrightarrow{a_1}$ и $\overrightarrow{a_2}$, normal to the parallel faces – as $\vec{n}$, normal to the spherical surface (1) – as $\overrightarrow{n_1}$. Obviously, $\overrightarrow{n_1}$ is defined by the expression

$$\vec{n}_1 = \{\frac{X}{R};\ \frac{Y}{R};\ \frac{z-\delta}{R}\} \tag{56}$$

where x ,y, and z – δ- coordinates of the surface, where normal is taken.

Determination of the beam angle doubling at the output of BL

Suppose that a monochromatic electromagnetic wave strikes through the front face of the lens in the form of a narrow beam at an arbitrary angle to the normal $\vec{n}$. Provided circular polarization of the incident wave refracted at the front edge, it is divided into two waves with linear polarization: the o and e-wave.

On a spherical surface, each of these waves in turn will be divided into two, so there will be four waves at the BL output in general. The intensity of the latter is defined by the relevant Fresnel coefficients on the front face and a spherical surface, and the BL output intensity for some waves may be very small.

It is obvious that the wave with the o-polarization passes BL without changing its original direction, while the other wave changes it.

Consider first the situation where in all BL intervals the wave has the e-wave polarization. Suppose that the propagation direction of the e-wave is defined by the unit vectors $\vec{k}_0$, $\vec{k}_1$, $\vec{k}_2$ and $\vec{k}_3$ in the intervals I, II, III and IV respectively. (Figure 5). The directions of these vectors are determined obviously from the boundary conditions at the interface in the ACL. A rigorous solution of this problem results in extremely cumbersome results, which are not suitable for physical analysis. Therefore, the authors suggest using the approximate calculation as in (Mayer, 2007), which is based upon the use of a small parameter.

$$\delta = \frac{n_e^2 - n_o^2}{n_o^2} \tag{57}$$

and the accuracy of the calculation is determined by the value δ^2. The error in this case (related to BL calculations) does not exceed 5-10%.

The method, developed in (38), gives the possibility to assert that the vectors $\vec{k}_1$, $\vec{k}_2$ and $\vec{k}_3$ can be expressed as:

$$\vec{K}_1 = \vec{K}_1^{(0)} + \delta \vec{K}_1^{(1)}$$

$$\vec{K}_1^{(0)} = \frac{\Delta - (\vec{n}\vec{k}_0)}{n_e}\vec{n} + \frac{1}{n_e}\vec{k}_0$$

$$\vec{K}_1^{(1)} = \frac{\left(\vec{K}_1^{(0)}\vec{a}_1\right)^2 (1-\left(\vec{K}_1^{(0)}\vec{n}\right)^2 \Delta\overline{(\vec{n}\vec{k}_0)})}{2n_e\Delta}\vec{n} - \frac{\left(\vec{K}_1^{(0)}\vec{a}_1\right)^2}{2n_e} \quad (58)$$

where $\Delta = \sqrt{n_e^2 - 1 + (\vec{n}\vec{k}_0)^2}$ and

$$\vec{K}_2 = \delta \frac{\left(\vec{K}_1^{(0)}\vec{a}_2\right)^2 - \left(\vec{K}_1^{(0)}\vec{a}_1\right)^2}{2\overline{(\vec{K}_1^{(0)}\vec{n})}}\vec{n}_1 + [1 - \delta \frac{\left(\vec{K}_1^{(0)}\vec{a}_2\right)^2 - \left(\vec{K}_1^{(0)}\vec{a}_1\right)^2}{2}]\vec{k}_1 \quad (59)$$

The vector $\vec{n_1}$ is measured at the intersection of the beam with a spherical surface, and it can be shown that

$$\vec{n}_1 = \frac{\vec{N}}{R} - \frac{\left(\vec{K}_1^{(0)}\vec{N}\right) + \sqrt{(\vec{K}_1^{(0)}\vec{N})^2 - K_1^{(0)2}(N^2 - R^2) sina}}{K_1^{(0)2}}\vec{K}_1^0 \quad (60)$$

where $\vec{N}$={$x_0, y_0 - \delta$} – the vector drawn from the center of the spherical boundaries within ACL to the entry point of the beam into the lens (see Figure 5), where $\delta > 0$ defines the beam incidence at the left of BL and $\delta < 0$ – defines the beam incidence at the right of BL (Figure 3).

Consequently,

$$\vec{k}_3 = d_3\vec{n} + \beta_3\vec{k}_2 \quad (61)$$

where

$$d_3 = (\vec{k}_o\vec{n}) - \Delta + \delta \frac{n_e(\vec{k}_o\vec{n})\left[\left(\vec{K}_1^{(0)}\vec{a}_2\right)^2 - \left(\vec{K}_1^{(0)}\vec{a}_1\right)^2\right]}{2\overline{(\vec{K}_1^{(0)}\vec{n})}(\vec{k}_o\vec{n})} - \delta \frac{n_e^2\left(\vec{K}_1^{(0)}\vec{a}_1\right)^2}{2\Delta}$$

$$\beta_3 = n_e - \delta \frac{\overline{(\vec{K}_1^{(0)}\vec{a}_2)}}{2} n_e \quad (62)$$

The angle between the initial direction of the beam and its ACL output direction is obviously determined by the relation $\cos\chi = (\vec{k}_0\vec{k}_3)$ or, keeping in mind its small values and with regard to (62)-(64) we obtain:

$$\chi = \frac{n_0^2 - n_e^2}{n_0^2} \frac{\left[\left(\vec{K}_1^{(0)}\vec{a}_2\right)^2 - \left(\vec{K}_1^{(0)}\vec{a}_1\right)^2\right]}{2(\vec{n}_1\vec{k}_1^0)(\vec{n}\vec{k}_0)} n_e \sqrt{(\vec{n}_1\vec{k}_0)^2 + (\vec{n}\vec{k}_0)^2 - 2(\vec{n}_1\vec{k}_1^0)(\vec{n}\vec{k}_0)(\vec{n}\vec{n}_1)} \quad (63)$$

In deriving the expression (63) the authors assume that the e - beam retains its polarization at the intersection of all BL borders. One can show however, that

(63) describes all possible polarization options. Thus, if the o-beam is transformed into the e-beam on a spherical surface, the dividing angle χ can be found using the expression (63), assuming that ($\vec{K}_1^{(0)}$, $\vec{a}_1$) =1. If the e-beam is transformed into the o-beam on the spherical surface, then the angle χ can be defined by (63), $(\vec{k}_1^{(0)}, \vec{a}_2) = 1$. In the case of the beam incidence on the entrance face of BL at an arbitrary angle, the wave vector of the beam is defined as follows:

$$\vec{K}_0 = \{sin\alpha cos\varphi; \quad sin\alpha sin\varphi; \quad cos\alpha\} \tag{64}$$

where λ- the angle between $\overrightarrow{K_0}$ and the axis OZ. The wave unit vector of the e-beam in the interval II is determined as follows:

$$\vec{K}_0 = \{\frac{sin\alpha cos\varphi}{n_e}; \quad \frac{sin\alpha sin\varphi}{n_e}; \quad \sqrt{1 - \frac{sin^2\alpha}{n_e^2}}\} \tag{65}$$

The value of the normal to the spherical surface is defined by the equation of the beam propagation in the interval II:

$$\frac{x_2 - x_1}{K_{1x}} = \frac{y_2 - y_1}{K_{1y}} = \frac{z_2 - z_1}{K_{1z}} \tag{66}$$

where x_1=d$cos\varphi$; y_1=d$sin\varphi$; z_1=0, coordinates of M_1. From (66) we obtain coordinates of M_2

$$x_2 = x_1 + \frac{k_{1x}}{k_{1z}} z_2 = \left[\frac{sin\alpha}{\sqrt{n_e^2 - sin^2\alpha}} z_2 + d\right] cos\varphi$$

$$y_2 = y_1 + \frac{k_{1y}}{k_{1z}} z_2 = \left[\frac{sin\alpha}{\sqrt{n_e^2 - sin^2\alpha}} z_2 + d\right] sin\varphi \tag{67}$$

Inserting the expression (67) into the equation of spherical surface (1), we obtain

$$z_2 - \delta = -\frac{1}{n_e^2}\left[\begin{array}{l} \sin\alpha\left(\delta\sin\alpha + d\sqrt{n_e^2 - \sin^2\alpha}\right) + \\ + \sqrt{n_e^2 - \sin^2\alpha}\, x \sqrt{R^2 n_e^2 - \left(\delta\sin\alpha + d\sqrt{n_e^2 - \sin^2\alpha}\right)^2} \end{array}\right] \tag{68}$$

From here we obtain

$$Z_2 = \frac{1}{n_e^2}\sqrt{n_e^2 - sin^2\alpha}[\left(\delta sin\alpha + d\sqrt{n_e^2 - sin^2\alpha} - dsin\alpha\right)$$
$$- \sqrt{R^2 n_e^2 - (\delta sin\alpha + d\sqrt{n_e^2 - sin^2\alpha})^2} \tag{69}$$

Considering (68), from (69) we obtain

$$x_2 = [\sqrt{n_e^2 - sin^2\alpha}\left[\frac{\left(\delta sin\alpha + d\sqrt{n_e^2 - sin^2\alpha} - dsin\alpha\right) -}{sin\alpha\sqrt{R^2 n_e^2 - (\delta sin\alpha + d\sqrt{n_e^2 - sin^2\alpha})^2}}\right]\frac{cos\varphi}{n_e^2}$$

$$Y_2 = [\sqrt{n_e^2 - sin^2\alpha}\left[\frac{\left(\delta sin\alpha + d\sqrt{n_e^2 - sin^2\alpha} - dsin\alpha\right)}{-sin\alpha\sqrt{R^2n_e^2 - (\delta sin\alpha + d\sqrt{n_e^2 - sin^2\alpha})^2}}\right]\frac{sin\varphi}{n_e^2} \tag{70}$$

Inserting the expressions (68) and (70) in (56), we obtain the expression for the normal to the spherical surface at the point M_2:

$$\vec{n}_1 = \frac{1}{Rn_e^2}\left\{\begin{array}{l} \left[\sqrt{n_e^2 - sin^2\alpha}\left(\delta sin\alpha + d\sqrt{(n_e^2 - sin^2\alpha} - sin\alpha\sqrt{R^2n_e^2 - \left(\delta sin\alpha + d\sqrt{n_e^2 - sin^2\alpha}\right)^2}\right)\right]\cdot \\ \cdot\cos\alpha\left[\sqrt{n_e^2 - sin^2\alpha}\left(\delta sin\alpha + d\sqrt{n_e^2 - sin^2\alpha} - sin\alpha\sqrt{R^2n_e^2 - \left(\delta sin\alpha + d\sqrt{n_e^2 - sin^2\alpha}\right)^2}\right)\right]\sin\varphi - \\ -\left[sin\alpha\left(\delta sin\alpha + d\sqrt{n_e^2 - sin^2\alpha} + \sqrt{n_e^2 - sin^2\alpha}\sqrt{R^2n_e^2 - \left(\delta sin\alpha + d\sqrt{n_e^2 - sin^2\alpha}\right)^2}\right)\right] \end{array}\right\} \tag{71}$$

Considering the expressions (64), (65) and (71), from (63), we obtain

$$\chi = \frac{\delta}{2}\left[\left(\vec{K}_1^{(0)}\vec{a}_2\right)^2 - \left(\vec{K}_1^{(0)}\vec{a}_1\right)^2\right]\left[tg\alpha - \frac{(\delta sin\alpha + d\sqrt{n_e^2 - sin^2\alpha})^2\sqrt{n_e^2 - sin^2\alpha}}{cos\alpha\sqrt{\left(R^2n_e^2 - (\delta sin\alpha + d\sqrt{n_e^2 - sin^2\alpha})^2\right)}}\right] \tag{72}$$

The formula (72) defines the dividing angle in the output of BL-1 and BL-2. For BL-2, the dividing angle for the (eo)-wave is defined as follows

$$\chi^0 = \frac{\delta}{2n_e^2}(sin^2\alpha cos^2\varphi - n_e^2)\mathrm{B} \tag{73}$$

where $\mathrm{B} = tg\alpha - \frac{(\delta sin\alpha + d\sqrt{n_e^2 - sin^2\alpha})^2\sqrt{n_e^2 - sin^2\alpha}}{cos\alpha\sqrt{\left(R^2n_e^2 - (\delta sin\alpha + d\sqrt{n_e^2 - sin^2\alpha})^2\right)}}$, for the (oe)-wave from (72) we obtain

$$\chi^e = \frac{\delta}{2n_e^2}(n_e^2 - sin^2\alpha sin^2\varphi) * \mathrm{B} \tag{74}$$

The (eo) wave in the BL-2 output is propagated as the o-wave, along the converging line, and the (oe) – wave in the BL-2 output is propagated as the e-wave along the diverging line. The dividing angle between these waves (e and o) in the output of BL-2 is determined as follows:

$$\chi^{e0} = \chi^e + (-\chi^0) = \frac{\delta}{2n_e^2}(2n_e^2 sin^2\alpha) * \mathrm{B} \tag{75}$$

At normal incidence of the beam on the front face of BL-2, in other words, provided $\alpha = 0$ the formula (75) takes a simple form:

$$\chi^{eo} = Sn_e\frac{d}{R} \tag{76}$$

This was previously obtained in (54), in other words, the linear dependence of the dividing angle between the (o) and (e) waves in the output of BL-2 on the radius vector d. The dependence of the dividing angle χ^{oe} on the incidence angle d is shown in Figures 7a and 7b. The dividing angle of the (oo) - wave with regard to (72) is expressed as follows

$$\chi^{oo} = 0 \tag{77}$$

Obviously, the direction of wave propagation does not depend on α.

For the (ee)-wave from (72) we obtain

$$\chi^{ee}=\frac{\delta}{2}sin^2\cos2\varphi\cdot B \quad (78)$$

Provided $\alpha=0$, or $\varphi=\frac{\pi}{4}$ from (78), we obtain $\chi^{ee}=0$.

The (oo) and (ee) waves are formed in the output of ACL-2 at high α values (α> 35˚). This is explained by the fact that full transformation of waves occurs on the spherical surface, in other words, the o-beam in the interval 2 is fully transformed into the e-beam in the interval 3 of BL-2, and e-beam in the interval 2 of the lens is fully transformed into the o-beam in the interval 3 of BL-2. Therefore, provided normal incidence of the beam on the BL-2 (α=0) or provided $\varphi\neq\frac{\pi}{4}$ and $\alpha\neq0$, two waves are formed with (oe) and (eo) polarization in the output of BL-2.

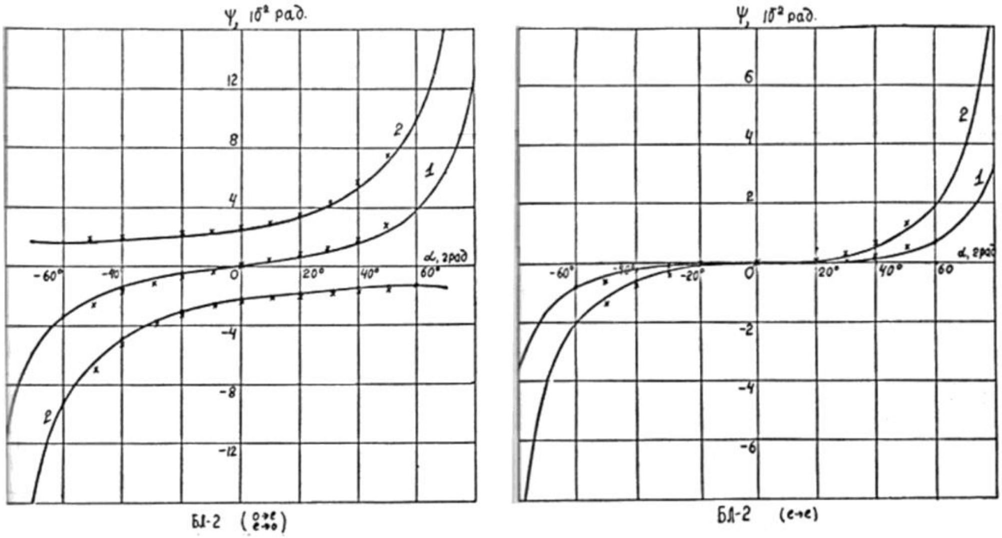

a) The angle between the (oe) and (eo) waves. Estimated dependence - unbroken line. Estimated and experimental dependencies differ only provided high angles of beam incidence (**α**)

b) The angle between the (oo) and (ee) waves. Estimated dependence - unbroken line. Estimated and experimental dependencies fully coincide.

Figure 7. Dependence of the dividing angle in the BL-2 on the angle of beam incidence on the output face. Experimental dependence - x (dots)

For the BL-1, the wave-dividing angle at the output of BL-1, is also defined by the formula (71).

For the (oo)-wave we obviously obtain $\chi^{oo}=0$

For the (oe)-wave, we obtain

$$\chi^{oe}=\frac{\delta}{2n_e^2}sin^2\alpha*B \quad (79)$$

The dividing angle of the (eo) and (ee) waves is determined as follows:

$$\chi^{oe}=\frac{\delta}{2n_e^2}(n_e^2-sin^2cos^2\varphi)*B \quad (80)$$

$$\chi^{ee}=\frac{\delta}{2n_e^2}(n_e^2-sin^2(1+cos^2\varphi))*B \quad (81)$$

Under α = 0, from (79) we obtain χ^{oe}=0. The expressions (80) and (79) provided d = 0 will take the following form:

$$\chi^{eo}=\chi^{ee}= - \frac{S}{2} n_e \frac{d}{R} \tag{82}$$

As is clear from (82), we obtain a linear dependence of the dividing angle of the (eo) and (ee) waves from the radius vector d, which was obtained earlier in the paraxial approximation (see (54)

The sign "-" in (83) means that that the (eo) and (ee) waves in the output of BL-1 are propagated by converging line.

The dependence of the dividing angle in BL-1 on the angle of incidence on BL-1 is shown in Figures 8a, 8b and in Figure 9 for two values of the radius vector d (d = 0; d = 4 mm).

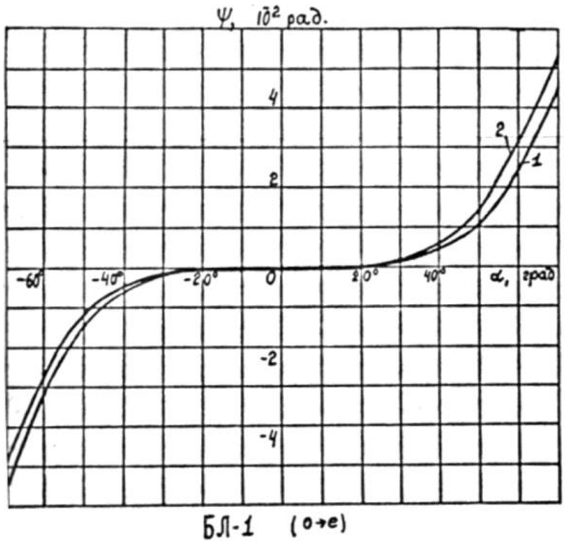

a) the angle between the (oo) and (oe) waves. Estimated dependence: 1- provided d=0, 2 - provided d=4 mm.

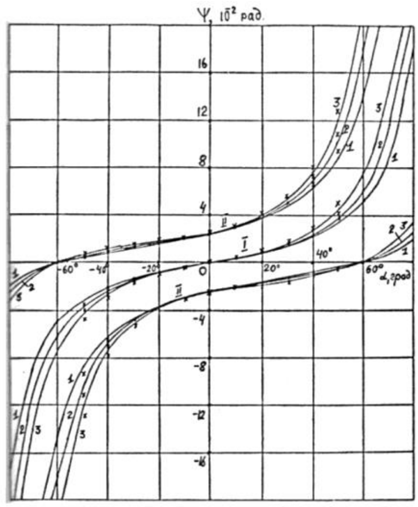

b) the angle between the (oe) and (eo) waves. Experimental dependence –x(dots). Estimated dependence – unbroken line 1- under d=0, $\varphi = \frac{\pi}{4}$; 2 - under d=4 mm, $\varphi = \frac{\pi}{2}$.

Figure 8. Dependence of the dividing angle in BL-1 on the angle of beam incidence on the output face. Experimental dependence - x (dots)

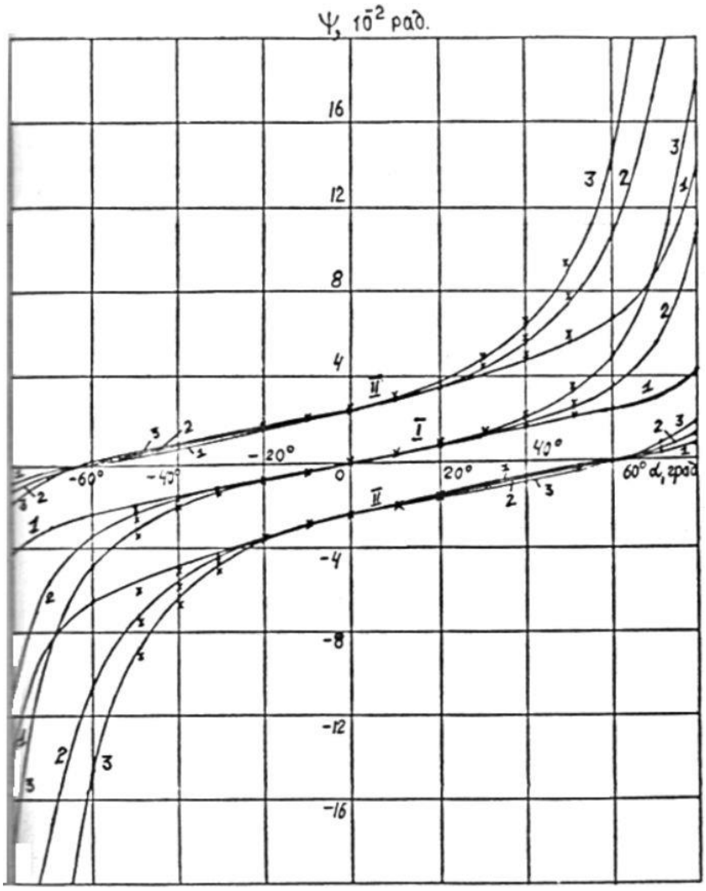

Figure 9. Dependence of the dividing angle in ACL-1/the angle between the oe and eo waves/ on the angle of beam incidence on the output face. Experimental dependence - x (dots). Calculated dependence - solid line

Implications and Recommendations

Pursuant to the well-known theory of electromagnetic waves propagation in isotropic and anisotropic crystals, rigorous calculation of beam propagation in a system consisting of several anisotropic crystals, results in cumbersome expressions that are not suitable for engineering calculations and do not provide the possibility to study general properties of the two-component crystal-optical lenses.

This article was based on paraxial approximation (narrow beam method) that provided the possibility to consider propagation of beams through the two-component crystal-optic lenses under various orientations of optical axes in their components.

The authors developed an effective method of calculating propagation of electromagnetic waves through the two-component crystal-optical lenses based on uniaxial Iceland spar crystals with different orientations of the optical axes of the crystals in the lens components.

The obtained expressions reflect all the main features of such systems provided arbitrary orientation of the optical axes in these lenses and are suitable for engineering calculations.

Based on the analysis of the obtained expression, the study offers constructive division of BL's into the BL-1 and BL-2 lens types, and consideration of the basic properties (including the focusing properties) of BL-1 and BL-2 lens types. The obtained expressions describe the beam path at the BL output in the case of a collimated laser beam; the calculation method of the known two-component crystal-optical systems was generalized.

The authors presented a comprehensive experimental study of crystal-optical lenses in a split mode of electromagnetic waves at the output of crystal-optical lenses.

The results of calculations by the above formulas are compared with experimental data. The study found a high agreement between the results of theoretical calculation with the experimental data, which proves correctness of the elaborated method aimed at calculating propagation of electromagnetic waves through the two-component crystal-optical lenses.

Disclosure statement

No potential conflict of interest was reported by the authors.

Notes on contributors

Abilhan U. Umbetov is a PhD, Dean of the Faculty of Natural Sciences and Information, Associate Professor of the Mathematics and Physics Department, Arkalyk State Pedagogical Institute named after Y. Altynsarin, Arkalyk, Kazakhstan.

Sania B. Zhumabaeva Holds a Master Degree at Mathematics and Physics Department, Arkalyk State Pedagogical Institute named after Y. Altynsarin, Arkalyk, Kazakhstan.

Anuza Zhakenova Holds a Master Degree at Mathematics and Physics Department, Arkalyk State Pedagogical Institute named after Y. Altynsarin, Arkalyk, Kazakhstan.

Bazargul S. Sadykova Holds a Master Degree at Mathematics and Physics Department, Arkalyk State Pedagogical Institute named after Y. Altynsarin, Arkalyk, Kazakhstan.

Anar K. Tulegenova Holds a Master Degree at Mathematics and Physics Department, Arkalyk State Pedagogical Institute named after Y. Altynsarin, Arkalyk, Kazakhstan.

Assel A. Aubakirova Holds a Master Degree at Mathematics and Physics Department, Arkalyk State Pedagogical Institute named after Y. Altynsarin, Arkalyk, Kazakhstan.

Saule Zh. Dzhaketova Holds a Master Degree at Mathematics and Physics Department, Arkalyk State Pedagogical Institute named after Y. Altynsarin, Arkalyk, Kazakhstan.

References

Alferov, S. V. (2014) Experimental generation of the longitudinal electric field component on the optical axis with high-numerical-aperture binary axicons. *Proceedings of the Optical Technologies for Telecommunications*, 9533, 95330A-95330D-6.

Arminjon, M. & Reifler, F. (2013) Equivalent Forms of Dirac Equations in Curved Space-time Generalized de Broglie Relations. *Brazilian Journal of Physics, 43(2),* 64-77.

Barkovskii, L. M. & Borzdov, G. N. (1975). Electromagnetic waves in absorbing plane-layered anisotropic and gyrotropic media. *Journal of Applied Spectroscopy*, *23(1),* 985-991.

Bazykin, S. (2014) *Information measuring systems based on interferenometers*. Penza: PSU. 132p.

Born, M. & Wolf, R. (1997) *Principles of Optics*. Cambridge: Cambridge Univ. Press. 987p.

Boyd, R. W. (2008) *Nonlinear Optics*. Nonlinear Optics. New York: Academic Press Inc. 620p.

Cattoor, R., Hönninger, I., Tondusson, M., Veber, P., Kalkandjiev, T., Rytz, D., Canion, L. & Eichhorn, M. (2014) Wavelength dependence of the orientation of optic axes in KGW. *Applied Physics B, 116(4),* 831-836.

Chang, W. (2005) *Principles of lasers and optics.* New York: Cambridge University Press. 262p.

Demtröder, W. (2013) *Laser spectroscopy: basic concepts and instrumentation*. Berlin: Springer Science & Business Media. 237p.

Fabrizio, D. & Rinaldi, D. (2015) Mechanical and Optical Properties of Anisotropic Single-Crystal Prisms. *Journal of Elasticity, 120,* 197-224.

Frieden, B. R. (2012). *Probability, statistical optics, and data testing*. New York: Dover Publications. 280p.

Harris, S. E. (1963) Conversion of fm light to am light using birefringent crystals. *Appl. Phys. Lett.*, *2(3),* 47-49

Khonina, S. N. (2013) Experimental demonstration of the generation of the longitudinal E-field component on the optical axis with high numerical – apertures binary axioms illuminated by linearly and circularly polarized beams. *Journal of Optics, 15(8),* 85704-85712

Khonina, S. N., Karpeev, S. V., Alferov, S. V. (2012) Polarization converter for higher-order laser beams using a single binary diffractive optical element as beamsplitter. *Opt.Lett.*, *37(12),* 2385-2387.

Konoshonkin, A. V., Kustova, N. V., Borovoi, A. G.. (2015) Beam-splitting code for light scattering by ice crystal particles within geometric-optics approximation. *Journal of Quantitative Spectroscopy and Radiative Transfer, 164*, 175-183.

Mayer, V. V. (2007) *Total internal reflection of light. Educational research.* Moscow: FIZMATLIT. 160p.

Osipov, Y. (1973) Polarized lenses with binary structure. *Optical-mechanical industry 5*, 5-7.

Porfiriyev, L. F. (2013) *Fundamentals of signal transformation theory in optical-electronic systems.* St. Petersburg: Lan. 387p.

Savin, A. V., Zubova, E. A. and Manevitch, L. I. (2005) Survival condition for low-frequency quasi-one-dimensional breathers in a two-dimensional strongly anisotropic crystal. *Physical Review 71,* 224-303.

Singh, B. K., Chaudhari, M. K., and Pandey, P. C. (2016) Photonic and Omnidirectional Band Gap Engineering in One-Dimensional Photonic Crystals Consisting of Linearly Graded Index Material. *Journal of Lightwave Technology, 34(10),* 2431-2438.

Tarasov, V. V., Torshina, I. P., Yakushenkov, Y. G. (2014) *Current problems in optical engineering. Modern optical engineering problems*. Moscow: MIIGAiK, 224 p.

Yang, J., Kim, G. H., Lee, B., Sall, E. G., Chizhov, S. A., Yashin, V. E., Kang U. (2015) Investigation of Thermooptical Effects in a High-brightness Yb:KGW Laser. *Proceedings of 2015 Conference on Lasers and Electro-Optics Pacific Rim*, *2*, 1-2.